DEVELOPMENT OF COLORED GLASS FROM DOPED WITH CuO AND Cr_2O_3 FOR USE AS ARTIFICIAL GEMSTONES AND JEWELRY

Sunantasak Ravangvong[1,*], Punsak Glumglomchit[2], Chayanut Pranpreechakul[2], Chaiyasit Kasorn[2], Thanabudee Hansapiromchock[2] and Kittisak Sriwongsa[3,4]

Received: August 14, 2025; Revised: November 10, 2025; Accepted: November 24, 2025

Abstract

This study focuses on investigation and development of low temperature glasses for application as synthetic gemstones and lead-free glass-based jewelry. The glass systems were primarily composed of waste glass (WG) and doped with copper oxide (CuO) and chromium oxide (Cr_2O_3). The glass systems were prepared using the melt quenching technique in the compositional formula (100-x)WG: xCuO/Cr_2O_3, where x = 0.0, 0.1, 0.2, 0.3, 0.4, and 0.5 mol%. The results found that the increasing of CuO and Cr_2O_3 content led to increase in both density and refractive index of glass systems. The analysis absorption spectra of CuO doped glass systems at 300-2000 nm, it found absorption peak at 800 nm ($^2E \rightarrow {}^2T_2$) due to Cu^{2+} ion in octahedral coordination with a strong tetragonal distortion. In case of Cr_2O_3 doped glass systems at absorption spectra 400-1000 nm, it found absorption peaks around 420, 690 and 635 nm, as corresponding to the $^4A_2 \rightarrow {}^4T_1(F)$, $^4A_{2g}(F) \rightarrow {}^4T_{2g}(F)$ and $^4A_{2g}(F) \rightarrow {}^2T_{1g}(F)$ transitions of Cr^{3+} ions, respectively. Colorimetric analysis based on the CIE L*a*b revealed that the CuO and Cr_2O_3 doped glass systems exhibited blue and green, respectively. These results demonstrate a sustainable way to recycle waste glass into value-added colored materials for eco-friendly jewelry applications.

Keywords: **Waste glasses; Artificial gems; Optical**

[1] *Division of Science and Technology, Faculty of Science and Technology, Phetchaburi Rajabhat University, Phetchaburi 76000, Thailand.*
[2] *Hua Hin Wittayalai School, Hua Hin, Prachuap Khiri Khan 77110, Thailand.*
[3] *Faculty of Education, Silpakorn University, Nakhon Pathom 73000, Thailand.*
[4] *The Demonstration School of Silpakorn University, Nakhon Pathom 73000, Thailand.*
[*] *Corresponding author*

DOI: https://doi.org/10.55766/sujst11214

Introduction

At Present, the growing global population has significantly increased the demand for infrastructure materials. This surge in demand has consequently led to a continuous increase in various types of waste. For example, household waste glass (WG) has increased by 5%. Additionally, countries like the USA, UK, Canada, and Turkey generate around 20, 3, 0.8, and 0.12 million tons of WG per year, respectively. According to a United Nations report, waste glass accounts for approximately 7% of 200 million tons of solid waste generated globally. To mitigate its environmental, safety, and health impacts, various efforts have been undertaken to recycle WG. These initiatives also contribute to the development of a circular economy through innovation and research, thereby advancing global sustainability (Bootkul *et al.*, 2017; Nasiru *et al.*, 2021; Hamada *et al.*, 2022; Salahaddin *et al.*, 2022; Sayyed *et al.*, 2022). Waste glass has been successfully utilized as a component in various materials, such as concrete (Adesina, 2022) and glass-ceramics (Liu *et al.*, 2022). Several studies have analyzed the composition of WG and found that silicon dioxide (SiO_2) is the predominant oxide, whereas transition m*etal* oxides are present in lower concentrations (Eid *et al.*, 2022; Silveira *et al.*, 2022; Tahwia *et al.*, 2022).

Glass is a material that can be fabricated from various oxide compounds, which are typically categorized into three functional groups: (1) glass network formers such as SiO_2, (2) modifiers use for improve the melting point etc. such as Na_2O and CaO, and (3) intermediates use for improve refractive index etc. such as Fe_2O_3, TiO_2 and WO_3 (Khazaalah *et al.*, 2022; Ravangvong *et al.*, 2022; Ravangvong *et al.*, 2023; Eke, 2024; Sriwongsa *et al.*, 2024; Gao *et al.*, 2025; Sriwongsa *et al.*, 2025). Among these, silicon dioxide (SiO_2) is one of the most common network formers and is widely used in numerous applications due to its excellent properties, such as high transparency, chemical stability, low thermal expansion coefficient, high-temperature resistance, and outstanding electrical insulation (Alomairy *et al.*, 2021; Li *et al.*, 2022). Many researchers have studied glasses doped with transition m*etal* oxides such as CuO and Cr_2O_3.

Copper, with the electron configuration $3d^{10}$ $4s^1$, is a transition m*etal* that exhibits two common oxidation states: monovalent (Cu^+) and divalent (Cu^{2+}). In silicate glasses, Cu^+ and Cu^{2+} ions are octahedrally coordinated and act as network modifiers. The cuprous ion (Cu^+, $3d^{10}$ $4s^2$) does not produce coloration, whereas the cupric ion (Cu^{2+}, $3d^9$ $4s^2$) absorbs light in the visible region and generates color (Wongsing *et al.*, 2012). Chromium, with the electron configuration $3d^5$ $4s^1$, can exist in multiple oxidation states, including Cr^{3+}, Cr^{4+}, Cr^{5+}, and Cr^{6+}. Among these, Cr^{3+} and Cr^{6+} ions doped into glass systems are responsible for color formation, which can be observed through UV-VIS spectroscopy (Meejitpaisan *et al.*, 2012; Moustafa *et al.*, 2013; Srisittipokakun & Kaewkhao, 2013).

This study, waste glasses doped with CuO and Cr_2O_3 were fabricated and their physical and optical properties were investigated. The glass compositions were prepared according to the formula (100-x)WG : xCuO/Cr_2O_3 (x = 0.0, 0.1, 0.2, 0.3, 0.4, and 0.5 mol%). The physical properties were evaluated in terms of density and refractive index (RI), while the optical properties were examined using optical spectra and CIE L*a*b* color coordinates for both glass systems. Furthermore, CuO and Cr_2O_3 doping was employed to produce colored glass suitable for artificial jewelry, thereby enhancing the value of WG.

Materials and Methods

This work, commonly available glass wastes (WG) are collected, cleaned with hot water at 100°C and crushed. After that, WG were doped with CuO and Cr_2O_3 and prepared using the composition (100-x)WG : xCuO/Cr_2O_3, where x = 0.0, 0.1, 0.2, 0.3, 0.4, and 0.5 mol%. Each batch weighed approximately 10 g and was fabricated using the melt-quenching technique. The mixtures were melted at 1200°C for 3 hours, then annealed at 500 °C for 3 hours, followed by cooling to room temperature. And then, cut and polished in size about $1 \times 1.5 \times 0.25$ cm^3 for further analysis, as exhibited in Figure 2 and Figure 3. The chemical composition of the WG samples was analyzed using an energy-dispersive X-ray fluorescence (XRF) spectrometer (Minipal-4, Panalytical). The structural characteristics of the glasses were confirmed using X-ray diffraction (XRD) using Shimazdu XRD-6100. The density of WG samples was estimated using 4-digit microbalance A&D HR-200 which according to the Archimedes method, with water as the immersion medium, according to Equation (1):

$$\rho = \frac{W_{\text{air}}}{W_{\text{air}}\text{-}W_{\text{water}}} \times \rho_{\text{water}} \tag{1}$$

here W_{air} and W_{water} are weight of sample in air and water, respectively which density of water is

1.0000 g/cm^3 (Kaewkhao & Limsuwan, 2012; Sayyed *et al.*, 2021).

The refractive index (RI) of WG glass samples was measured at The Center of Excellence in Glass Technology and Materials Sciences (CEGM) is a specialize research center in Nakhon Pathom Rajabhat University (NPRU) at 25°C using an Abbe refractometer (ATAGO-3T). Additionally, their optical spectra were analyzed using a UV-Visible spectrophotometer (Cary-50).

Results and Discussion

The chemical compositions of the WG samples were analyzed using X-ray fluorescence (XRF) spectrometry, as shown in Table 1. The results revealed that SiO_2, a primary glass network former, is the main component, while transition m*etal* oxides are present in lower concentrations.

Table 1. The chemical composition of WG

Chemical composition (wt%)					
SiO_2	Na_2O	CaO	TiO_2	Fe_2O_3	WO_3
74.878	11.947	12.867	0.093	0.171	0.041

The X-ray diffraction pattern (XRD) of WG was displayed in Figure 1. The absence of sharp magnitudes and shown one board band peaks around 0-10° reflects amorphous characteristics (Sayyed *et al.*, 2021).

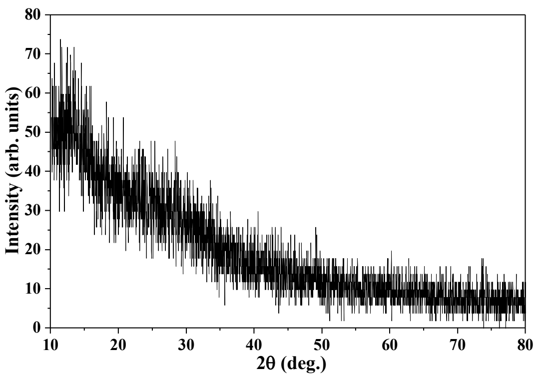

Figure 1. The XRD for WG

The colors of the WG glass samples doped with CuO and Cr_2O_3 are shown in Figure 2 and Figure 3. The CuO-doped samples exhibited a light blue color, while the Cr_2O_3-doped samples showed a greenish-yellow color. In both systems, the color intensity increased with higher concentrations of CuO and Cr_2O_3 respectively (Meejitpaisan *et al.*, 2012; Wongsing *et al.*, 2012; Srisittipokakun *et al.*, 2017).

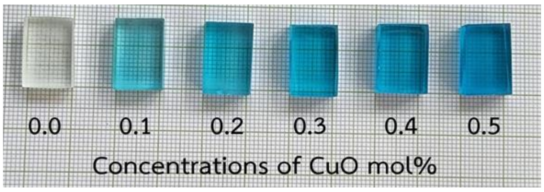

Figure 2. Glass samples of CuO doped WG system

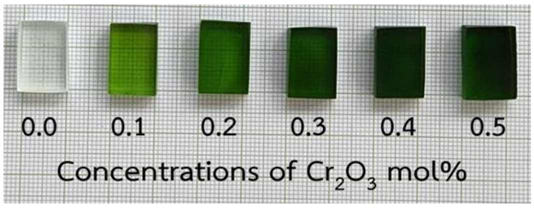

Figure 3. Glass samples of Cr_2O_3 doped WG system

The density values of the CuO- and Cr_2O_3-doped WG glass systems are presented in Figure 4 and Figure 5, respectively. The results show that density for both glass systems increased with higher CuO and Cr_2O_3 content. This trend is due to substitution of SiO_2 by CuO and Cr_2O_3, which possess higher molecular weights than SiO_2. As a result, the average molecular weight of the glass systems increased, leading to higher overall density (Srisittipokakun & Kaewkhao, 2013).

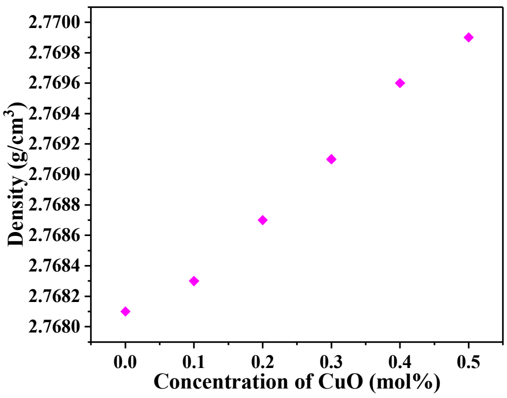

Figure 4. The density of CuO doped glass samples

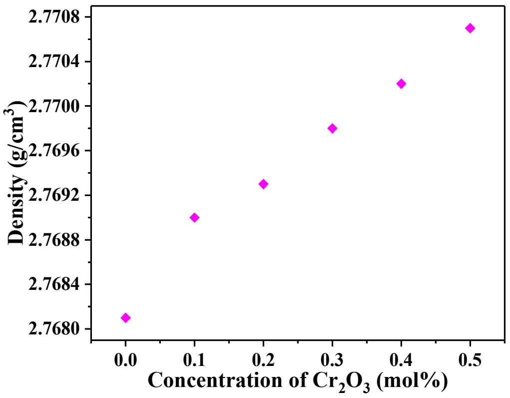

Figure 5. The density of Cr_2O_3 doped glass samples

The refractive index (RI) values for the CuO- and Cr_2O_3-doped WG glass systems are shown in Figure 6 and Figure 7, respectively. The RI of both glass systems increased with higher concentrations of CuO and Cr_2O_3. This behavior correlates with the increase in density; as the density of glass increases, the structure becomes more compact. This compaction reduces the velocity of light within the glass, resulting in a higher refractive index. In addition, this result can explain on the strength of Cu-O and Cr-O bond increased, that occur intense field around Cu^{2+} and Cr^{3+} ions (Srisittipokakun *et al.*, 2011; Srisittipokakun *et al.*, 2017; Glumglomchit *et al.*, 2018).

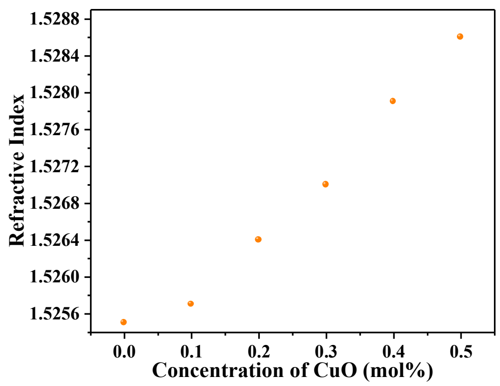

Figure 6. The RI of CuO doped glass system

The optical absorption spectra of CuO doped WG glass system at wavelength 300-2,000 nm were recorded and displayed in Figure 8. It found that the absorption bands near 800 nm from Cu^{2+}. This event is due to the energy transferred from $^2E_g(D) \rightarrow {}^2T_{2g}(D)$ in the glass matrices which Cu^{2+} ion in octahedral coordination with a strong tetragonal distortion (Srisittipokakun *et al.*, 2017).

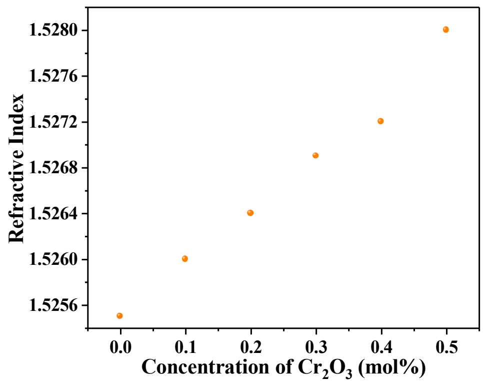

Figure 7. The RI of Cr_2O_3 doped glass system

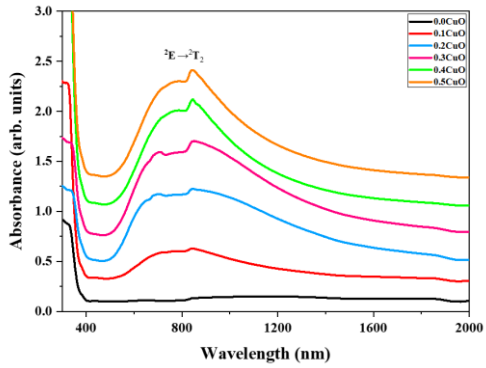

Figure 8. The optical spectra of CuO doped glass system

The spectra of Cr_2O_3 doped WG glass systems at wavelength 400-1,000 nm at room temperature as exhibited in Figure 9. It found absorption bands around wavelength near 420, 635 and 690 nm due to $^4A_2 \rightarrow {}^4T_1(F)$, $^4A_2g(F) \rightarrow {}^4T_2g(F)$ and $^4A_2g(F) \rightarrow {}^2T_1g(F)$ transition which arises from Cr^{3+} ions, respectively (Srisittipokakun & Kaewkhao 2013; Boonin *et al.*, 2021; Vinay *et al.*, 2025).

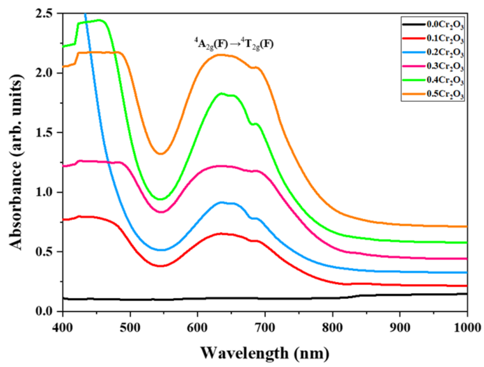

Figure 9. The optical spectra of Cr_2O_3 doped glass system

The CIE L*a*b* colour coordinates of the CuO- and Cr_2O_3-doped WG glass systems are presented in Table 2 and Table 3, and illustrated in Figure 10 and Figure 11, respectively. It was observed that both undoped glass systems appeared colourless. As the concentrations of CuO and Cr_2O_3 increased, the brightness (L*) values range from 40.4926 to 58.1600, a* values range from -23.5899 to 4.4585 and b* values around -21.4621 to 2.4585 for CuO-doped samples, while L* values range from 43.8690 to 67.3441, a* values range from -46.3505 to 0.2716 and b* values around from 2.4585 to 68.5794 for Cr_2O_3-doped samples. The L* values do not vary consistently with concentration because the optical behavior of real samples is complex, affected by light scattering, surface effects, and nonlinearity. In addition, the increasing CuO content, the WG glass system gave dark blue colour while gave green-yellow colour when increased Cr_2O_3 content in WG glass system. It can be seen that the more CuO and Cr_2O_3 content, the color of the glass will become darker. The color of CuO -doped glass system was according to the absorption spectra visible at 800 nm. While Cr_2O_3-doped glass system was according to the absorption spectra visible at 430 nm, 635 and 690 nm.

Table 2. CIE L*a*b of CuO doped glass samples

CuO (mol%)	L*	a*	b*
0.0	43.8690	0.2716	2.4585
0.1	58.1600	-7.5395	-3.7506
0.2	51.8139	-11.5984	-7.3799
0.3	40.4926	-13.8962	-9.6631
0.4	56.8710	-20.2836	-17.9494
0.5	58.8849	-23.5899	-21.4621

Table 3. CIE L*a*b of Cr_2O_3 doped glass samples

Cr_2O_3 (mol%)	L*	a*	b*
0.0	43.8690	0.2716	2.4585
0.1	67.3441	-27.7228	60.4130
0.2	61.0164	-37.2307	67.8545
0.3	49.3987	-38.3402	68.5794
0.4	47.6361	-46.3505	67.9904
0.5	46.3696	-43.4954	64.2529

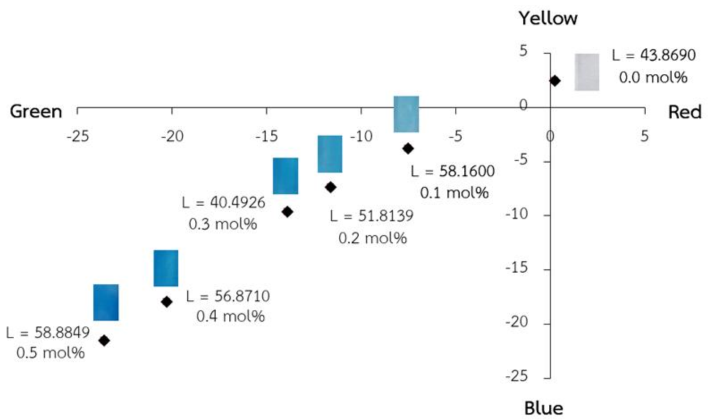

Figure 10. The L*a*b* of CuO doped glass system

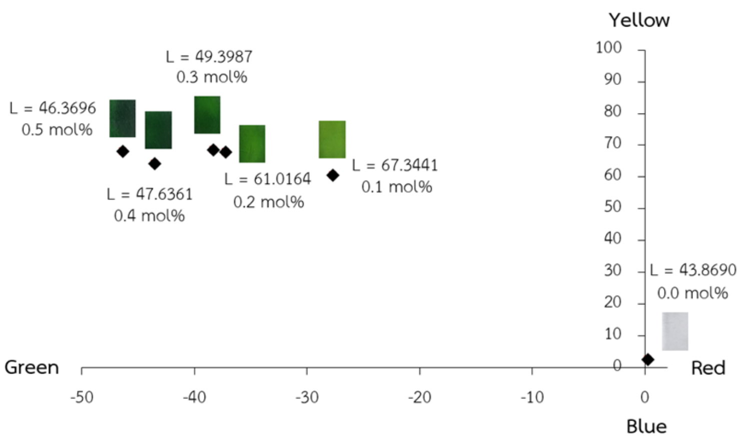

Figure 11. The L*a*b* of Cr_2O_3 doped glass system

Conclusions

The two-glass systems for CuO and Cr_2O_3 doped WG with composition (100-x) waste glasses: x CuO/Cr_2O_3 (x = 0.0, 0.1, 0.2, 0.3, 0.4 and 0.5 mol%) were synthesized using the melt-quenching technique. The two-glass systems are separately examined for their physical and optical properties. The density and refractive index for two-glass systems increased with increasing CuO and Cr_2O_3 concentrations. The absorption spectra revealed that CuO exhibited a band near 800 nm, the energy transferred from $^2E_g(D) \rightarrow {}^2T_{2g}(D)$ in the glass matrices while Cr_2O_3 showed absorption bands around 420, 635 and 690 nm, the energy transferred from $^4A_2 \rightarrow {}^4T_1(F)$, $^4A_{2g}(F) \rightarrow {}^4T_{2g}(F)$ and $^4A_{2g}(F) \rightarrow {}^2T_{1g}(F)$ transition which arises from Cr^{3+} ions, respectively. The brightness for two-glass systems were decreased with increasing CuO and Cr_2O_3 concentration. The CuO and Cr_2O_3 doped glass systems were given dark blue and green - yellow colour, respectively. These findings demonstrate that WG can be successfully recycled into glass suitable for artificial gem production, with tunable colors depending on the dopant type and concentration.

Acknowledgment

The authors would like to thank Thailand Science Research and Innovation (TSRI) National Science, Research and Innovation Fund (NSRF) to financially supported for this work.

References

Adesina, A. (2022). Durability and microstructural characteristics of alkali activated materials made with waste glass as precursor: A review. *Cleaner Materials, 6*, 100134. https://doi.org/10.1016/j.clema.2022.100134

Alomairy, S., Al-Buriahi, M. S., Wahab, E. A. A., Sriwunkum, C., & Shaaban, K. (2021). Synthesis, FTIR, and neutron/charged particle transmission properties of Pb_3O_4-SiO_2-ZnO-WO_3 glass system. *Ceramics International, 47*(12), 17322-17330. https://doi.org/10.1016/j.ceramint.2021.03.045

Boonin, K., Yamsuk, Y., Yasaka, P., & Kaewkhao, J. (2021). Red emission glass from Mn^{2+} doped in zinc barium aluminoborate glasses. *Materials Today: Proceedings, 43*(3), 2475-2483. https://doi.org/10.1016/j.matpr.2020.04.606

Bootkul, D., Kulrat, N., Dangtip, S., & Intarasiri, S. (2017). Development of glass-ceramics from soda lime silica glass waste by sintering method for opal imitation. *Materials Today: Proceedings, 4*(5), 6043-6050. https://doi.org/10.1016/j.matpr.2017.06.092

Eid, M. S., Bondouk, I. I., Saleh, H. M., Omar, K. M., Sayyed, M. I., El-Khatib, A. M., & Elsafi, M. (2022). Implementation of waste silicate glass into composition of ordinary cement for radiation shielding applications. *Nuclear Engineering and Technology, 54*(4), 1456-1463. https://doi.org/10.1016/j.net.2021.10.007

Eke, C. (2024). The role of WO_3 on the optical and radiation attenuation characteristics of ZnO-Na_2O-B_2O_3 glasses. *Radiation Physics and Chemistry, 224*, 112036. https://doi.org/10.1016/j.radphyschem.2024.112036

Gao, J., Si, X., Jiang, H., Yang, H., Zhang, W., Li, C., Qi, J., & Cao, J. (2025). Effect of TiO_2 on crystallization and sealing behavior of Na_2O-K_2O-TiO_2-SiO_2-Al_2O_3-ZnO glass sealant for PCFCs. *Ceramics International, 51*(12), 15857-15866. https://doi.org/10.1016/j.ceramint.2025.01.423

Glumglomchit, P., Rajagukguk, A., Kaewkhao, J., & Kirdsiri, K. (2018). Physical and optical investigation of lutetium-sodium-borate glasses. *Materials Today: Proceedings, 5*, 15054-15060. https://doi.org/10.1016/j.matpr.2018.04.056

Hamada, H., Alattar, A., Tayeh, B., Yahaya, F., & Thomas, B. (2022). Effect of recycled waste glass on the properties of high-performance concrete: A critical review. *Case Studies in Construction Materials, 17*, e01149. https://doi.org/10.1016/j.cscm.2022.e01149

Kaewkhao, J., & Limsuwan, P. (2012). Utilization of rice husk fly ash in the color glass production. *Procedia Engineering, 32*, 670-675. https://doi.org/10.1016/j.proeng.2012.01.1325

Khazaalah, T. H., Mustafa, I. S., Aloraini, D. A., Hisam, R., Zaid, M. H. M., Halimah, M. K., Sayyed, M. I., Malik, M. F. I. A., Almuqrin, A. H., Ezra, N. S., & Naeem, H. S. (2022). Investigation of optical properties and radioactive attenuation parameters of doped tungsten oxide soda lime silica SLS waste glass. *Journal of Materials Research and Technology, 19*, 3355-3365. https://doi.org/10.1016/j.jmrt.2022.05.178

Li, H., Yi, R., & Chen, C. (2022). Microstructure and mechanical performance of dissimilar material joints of 2024Al and SiO_2 glass by ultrasonic assisted soldering with Cu interlayer. *Journal of Materials Research and Technology, 18*, 3227-3239. https://doi.org/10.1016/j.jmrt.2022.03.155

Liu, Y., Wan, W., Yang, F., Hu, C., Liu, Z., & Wang, F. (2022). Performance of glass-ceramic-based lightweight aggregates manufactured from waste glass and muck. *Ceramics International, 48*(16), 23468-23480. https://doi.org/10.1016/j.ceramint.2022.04.342

Meejitpaisan, P., Kaewkhao, J., Limsuwan, P., & Kedkaew, C. (2012). Physical and optical properties of the SLS glass doped with low Cr_2O_3 concentrations. *Procedia Engineering, 32*, 787-792. https://doi.org/10.1016/j.proeng.2012.02.013

Moustafa, F. A., Fayad, A. M., Ezz-Eldin, F. M., & El-Kashif, I. (2013). Effect of gamma radiation on ultraviolet, visible and infrared studies of NiO, Cr_2O_3 and Fe_2O_3-doped alkali borate glasses. *Journal of Non-Crystalline Solids, 376*, 18-25. https://doi.org/10.1016/j.jnoncrysol.2013.04.052

Nasiru, S., Jiang, L., Yu, L., Chu, H., Huang, Y., Pei, C., Gu, Y., Jin, W., Klu, E. E., & Guo, M. Z. (2021). Properties of cement mortar containing recycled glass and rice husk ash. *Construction and Building Materials, 299*, 123900. https://doi.org/10.1016/j.conbuildmat.2021.123900

Ravangvong, S., Sriwongsa, K., Glumglomchit, P., Phamornsut, K., Yampichai, N., Tantiwatcharakultorn, A., Sangngoen, S., & Kaewkhao, J. (2022). Behaviors of TeO_2-B_2O_3-WO_3 glass system for ionizing radiation shielding performance: Photon, protons and alpha particles. *Materials Today: Proceedings, 65*(4), 2269-2276. https://doi.org/10.1016/j.matpr.2022.04.005

Ravangvong, S., Wattana, W., Khobkham, C., Sriwongsa, K., Glumglomchit, P., Sringam, R., Thongbangbai, A., Ruangtaweep, Y., & Kaewkhao, J. (2023). Fe_2O_3- and

MnO_2-doped waste glasses for artificial gems products. *Integrated Ferroelectrics, 238*, 262-270. https://doi.org/10.1080/10584587.2023.2234574

Salahaddin, S. D., Haido, J. H., & Wardeh, G. (2022). The behavior of UHPC containing recycled glass waste in place of cementitious materials: A comprehensive review. *Case Studies in Construction Materials, 17*, e01494. https://doi.org/10.1016/j.cscm.2022.e01494

Sayyed, M. I., Alrashedi, M. F., Almuqrin, A. H., & Elsafi, M. (2022). Recycling and optimizing waste lab glass with Bi_2O_3 nanoparticles to use as a transparent shield for photons. *Journal of Materials Research and Technology, 17*, 2073-2083. https://doi.org/10.1016/j.jmrt.2022.01.113

Sayyed, M. I., El-bashir, B. O., Alhuthali, A. M. S., Alajerami, Y. S. M., Al-Hadeethi, Y., & Mhareb, M. H. A. (2021). Gamma radiation shielding and structural features for barium strontium boro-tellurite glass modified with various concentrations of molybdenum oxide. *Journal of Non-Crystalline Solids, 559*, 120658. https://doi.org/10.1016/j.jnoncrysol.2021.120658

Silveira, N. C. G., Martins, M. L. F., Bezerra, A. C. S., & Araújo, F. G. S. (2022). Ecological geopolymer produced with a ternary system of red mud, glass waste, and Portland cement. *Cleaner Engineering and Technology, 6*, 100379. https://doi.org/10.1016/j.clet.2021.100379

Srisittipokakun, N., & Kaewkhao, J. (2013). Effect of co-doped Fe_2O_3 with MnO_2 ions in soda lime silicate glasses. *Materials Today: Proceedings, 4*(5), 6534-6539. https://doi.org/10.1016/j.matpr.2017.06.164

Srisittipokakun, N., Kirdsiri, K., Kaewkhao, J., Kedkaew, C., & Limsuwan, P. (2011). Absorption and coloration of MnO_2 doped in soda-lime-silicate and soda-lime-borate glasses. *Procedia Engineering, 8*, 261-265. https://doi.org/10.1016/j.proeng.2011.03.048

Srisittipokakun, N., Ruangtaweep, Y., Rachniyom, W., Boonin, K., & Kaewkhao, J. (2017). CuO, MnO_2 and Fe_2O_3 doped biomass ash as silica source for glass production in Thailand. *Results in Physics, 7*, 3449-3454. https://doi.org/10.1016/j.rinp.2017.09.010

Sriwongsa, K., Glumglomchit, P., Ardmad, R., Kaewkoed, A., Lakkaew, W., Ravangvong, S., & Chaiphaksa, W. (2025). Optical properties improvement of steel slag glass and their ionizing radiation and neutron shielding properties. *Suranaree Journal of Science and Technology, 32*(1), 030276(1-10). https://doi.org/10.55766/sujst9262

Sriwongsa, K., Ravangvong, S., Glumglomchit, P., Kaewjaeng, S., Intachai, N., Kothan, S., Mutuwong, C., & Kaewkhao, J. (2024). The investigation of physical, optical, X/gamma-rays and thermal neutron shielding properties using experimental, simulation, and theoretical for BaO-based glass system. *Radiation Physics and Chemistry, 222*, 111841. https://doi.org/10.1016/j.radphyschem.2024.111841

Tahwia, A. M., Heniegal, A. M., Abdellatief, M., Tayeh, B. A., & Elrahman, M. A. (2022). Properties of ultra-high performance geopolymer concrete incorporating recycled waste glass. *Case Studies in Construction Materials, 17*, e01393. https://doi.org/10.1016/j.cscm.2022.e01393

Vinay, D., Devaraja, C., & Utpal, D. (2025). A comprehensive review of structural, and optical properties of boronated glasses doped with 3-d transition metal oxides (TMOs). *Journal of Alloys and Compounds, 1024*, 180145. https://doi.org/10.1016/j.jallcom.2025.180145

Wongsing, T., Kaewkhao, J., Limsuwan, P., & Kedkaew, C. (2012). Formation and optical absorption of CuO-doped SLS system. *Procedia Engineering, 32*, 807-813. https://doi.org/10.1016/j.proeng.2012.02.016